# Magnetic properties of $NpPd_3$ and $PuPd_3$ intermetallic compounds*

W. J. Nellis,† A. R. Harvey,‡ G. H. Lander, B. D. Dunlap, M. B. Brodsky, M. H. Mueller, J. F. Reddy, and G. R. Davidson
*Argonne National Laboratory, Argonne, Illinois 60439*
(Received 1 August 1973)

Magnetization, electrical-resistivity, Mössbauer-effect, and neutron-diffraction measurements have been made between 1.5 and 300 °K for two phases of $NpPd_3$ and for $PuPd_3$. The compounds $PuPd_3$ and cubic $NpPd_3$ have the $AuCu_3$-type crystal structure. Hexagonal $NpPd_3$ has the $TiNi_3$-type structure and is the room-temperature equilibrium phase. Cubic $NpPd_3$ can be retained by rapid quenching, and the specimen used in this investigation has a long-range order parameter of $S = 0.92$. The cubic $NpPd_3$ compound is antiferromagnetic with a Néel temperature $T_N = (55 \pm 1)$ °K, and the magnetic transition is apparently first order, since the sublattice magnetization is constant up to 45 °K. A large energy gap $\Delta$ in the spin-wave dispersion relation is observed below 40 °K in the electrical resistivity with $\Delta \simeq 3k\,T_N \simeq k\Theta \simeq k(150\,°\text{K})$, where $\Theta$ is the Debye temperature obtained from the resistivity data. Cubic $PuPd_3$ is antiferromagnetic below 24 °K. Cubic $NpPd_3$ and $PuPd_3$ have a magnetic structure that consists of ferromagnetic (111) planes coupled antiferromagnetically, and they have ordered moments of $(2.0 \pm 0.1)\ \mu_B$/Np atom and $(0.8 \pm 0.1)\ \mu_B$/Pu atom, respectively. Hexagonal $NpPd_3$ does not possess long-range magnetic order, but does appear to have an abrupt transition to short-range magnetic order distributed throughout the bulk below $\sim$32 °K, as indicated by an apparent Curie temperature in the magnetization, a spin-disorder resistivity anomaly, and a broadening of the paramagnetic Mössbauer line as the temperature is lowered from 30 to 4.2 °K. Both $NpPd_3$ phases have the same effective paramagnetic moment of 2.74 $\mu_B$/Np atom, consistent with the $Np^{3+}$ ionic configuration, the same volume per formula unit, and essentially the same first- and second-nearest-neighbor neptunium environment. The difference in magnetic behavior between the cubic and hexagonal phases of $NpPd_3$ is at present not understood.

## I. INTRODUCTION

The understanding of the magnetic properties of the actinide metals and intermetallic compounds has proved to be relatively difficult, despite a wealth of experimental work. In contrast to both the 3*d* electrons which, in the transition series, are unshielded from neighboring atoms and readily form bands, and the well-localized 4*f* electrons of the rare-earth series, the 5*f* electrons possess characteristics of the transition and rare-earth series because of their intermediate extent in real space. In addition, the 5*f* and 6*d* electrons hybridize strongly in the early part of the actinide series, giving rise to broad energy bands[1] with a width of ~2 eV and no magnetic moments. Recently, a model involving spin fluctuations has been proposed to explain the nearly magnetic behavior of neptunium and plutonium.[2] Localized 5*f* moments are found on actinide ions *only* if the ions are further apart than a critical distance (~3.2–3.5 Å).[3] When the ions are well separated, we should expect the situation to resemble that in the rare-earth compounds, in which the magnetic properties are largely determined by the competition between the exchange and crystal-field interactions. Such interactions in rare-earth compounds have been well documented over the past few years,[4] and quantitative agreement has been obtained between theory and experiment. Unfortunately, no such detailed analysis has been successful in explaining the magnetic properties of any actinide intermetallic compound.

As part of a program aimed at looking at the $APd_3$ compounds (where $A$ = U, Np, and Pu), we present magnetic-suceptibility, electrical-resistivity, Mössbauer-effect, and neutron-diffraction results on two phases of $NpPd_3$ and on $PuPd_3$. The motivation for choosing the $Pd_3$ series stems basically from three reasons. (i) Neptunium has a localized moment, and plutonium is nearly magnetic in dilute palladium alloys. However, no magnetic ordering occurs in these solid solutions with actinide concentrations up to 13 at.%.[5] Hence, these intermetallic compounds were investigated to determine if the increased actinide concentration and the atomic order would induce magnetic ordering. Cubic $NpPd_3$ and $PuPd_3$ do indeed order antiferromagnetically, whereas hexagonal $NpPd_3$ does not possess long-range magnetic order.[6] (ii) All compounds have the simple cubic $AuCu_3$ ($L1_2$) structure or a simple hexagonal derivative, the $TiNi_3$ ($DO_{24}$) structure.[7] In both structure types the nearest actinide-actinide separation is large (~4.1 Å), and, on the basis of our earlier discussion, we should expect localized 5*f* electron behav-

ior with this cation separation. (iii) The magnetic properties of the corresponding rare-earth–$Pd_3$ series have been thoroughly investigated,[8,9] and are understood in terms of crystal-field theory. In fact, in these compounds the crystal-field effects are stronger than the magnetic interactions.

The first member of the series $UPd_3$, and its solid solutions with $ThPd_3$, have been the subject of magnetic-susceptibility[10] and electron-paramagnetic-resonance (EPR)[11] experiments. For low uranium concentrations in $ThPd_3$, the effective magnetic moment is 3.35 $\mu_B$ per U atom, which is close to the value of 3.58 $\mu_B$ expected from a $^3H_4$; $5f^2$ configuration. This implies that the ionic state of the uranium ion is $U^{4+}$. For uranium concentrations higher than 10 at.% in $ThPd_3$, the effective magnetic moment is 2.6 $\mu_B$ per U atom. A deviation from the Curie law occurs at ~100 °K for all uranium concentrations, but there is no indication of magnetic ordering in the $1/\chi$-vs-$T$ plots. The results of the EPR experiments[11] indicate that a simple crystal-field model is not applicable to $UPd_3$, and the authors suggest that a compensated spin state may exist in the uranium compound. Such a model explains both the susceptibility and EPR measurements, although the more recent concept of spin fluctuations is probably a more appropriate model.[12]

In general, the understanding of the magnetic behavior of actinide intermetallics is a formidable task. For example, Buschow and van Daal[13] and Mulak and Misiuk[14] have measured the magnetic susceptibility of the $UX_3$ series ($X$=Ga, In, Si, Ge, and Sn), all of which have the cubic $AuCu_3$ structure. Although the experimental results from both groups are similar, the interpretations discussed by the authors have little in common. Buschow and van Daal[13] have discussed their results in terms of a localized-spin-fluctuation model, whereas Mulak and Misiuk[14] have used a straightforward crystal-field approach, assuming that the electrostatic crystal-field potential acts on an integral number (2) of $5f$ electrons. However, by performing a number of experiments with different techniques on carefully prepared samples, we hope to encourage at least a phenomenological approach to their understanding. One advantage in employing a variety of experimental techniques is that false assumptions can be frequently eliminated, since a model that accounts for some experimental results is often inadequate for others.

## II. EXPERIMENTAL DETAILS

### A. Sample preparation

All samples have been prepared from high-purity elements, and no traces of impurity phases were detected in the x-ray powder patterns. As reported previously,[7] $NpPd_3$ exists in two phases. The equilibrium phase at room temperature has the hexagonal $TiNi_3$ ($D0_{24}$) structure. A sample of this phase was obtained by arc melting neptunium and palladium together in the correct proportions, annealing at 1350 °C for 85 h (or longer), and slowly cooling. The x-ray diffraction patterns indicated that the material was single phase with $a$ = (5.767 ± 0.001) Å and $c$ = (9.544 ± 0.001) Å. Cubic $NpPd_3$, which has the $AuCu_3$ ($L1_2$) structure with $a$ = (4.095 ± 0.001) Å, was obtained by rapidly cooling the arc-melted button of $NpPd_3$. Traces of hexagonal $NpPd_3$ were observed in the x-ray patterns of all but a few batches of cubic $NpPd_3$. The stable phase of $UPd_3$ is the $TiNi_3$ structure,[7] i.e., isostructural with hexagonal $NpPd_3$, with $a$ = 5.770 Å and $c$ = 9.648 Å. The stable phase of $PuPd_3$ is the $AuCu_3$ structure,[7] i.e., isostructural with cubic $NpPd_3$, with $a$ = (4.105 ± 0.001) Å. Samples of both compounds were obtained in a manner similar to the preparation of hexagonal $NpPd_3$ described above. An initial hope in the investigation was that $UPd_3$ and $PuPd_3$ might be stable in both the hexagonal and cubic forms. Unfortunately, no success was achieved in attempting to produce cubic $UPd_3$ by rapid quenching from the melt or to produce hexagonal $PuPd_3$ by annealing for many weeks.

### B. Experimental techniques

Electrical-resistivity measurements were made between 1.5 and 300 °K using a standard dc four-probe technique.[15] Magnetization measurements from 1.8 to 300 °K were made using the Faraday method.[16] The susceptibilities $\chi = M/H$ were obtained by taking data at six (or more) fields up to 14.5 kOe, fitting the results to a two-term equation (linear in $1/H$), and extrapolating to $1/H = 0$. Hyperfine spectra were obtained between 4.2 and 78 °K using the 59.6-keV Mössbauer resonance of $^{237}Np$ with a source of $^{241}Am$ in $\alpha$-Am metal. Procedures and techniques are similar to those previously described.[17] Neutron-diffraction patterns were obtained at the CP-5 Research Reactor with a conventional two-axis diffractometer. Neutrons were reflected from the (111) planes of a pressed germanium crystal to give a monochromatic beam of 1.20 Å. The samples of hexagonal (2.1 g) and cubic (1.8 g) $NpPd_3$ were contained in $\frac{1}{4}$-in.-diam vanadium capsules. In the case of $PuPd_3$, however, experiments were performed with the $^{239}Pu$ isotope, which has a high absorption cross section (750 b at 0.055 eV). For this experiment a special vanadium tube with an oval cross section (maximum dimensions 3.5×9 mm) was constructed and filled with 3.7 g of $PuPd_3$. A satisfactory signal was obtained by working in transmission through the thinner section. The over-all transmission of the incident beam was 0.19, and absorption corrections were applied.

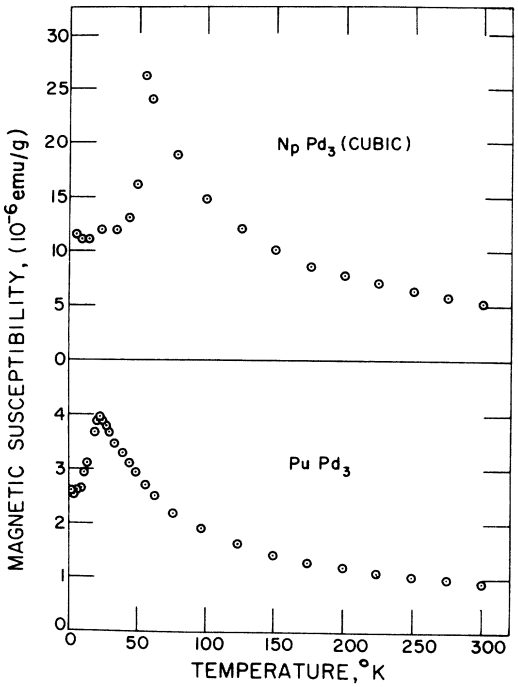


FIG. 1. Magnetic susceptibilities of cubic $NpPd_3$ and $PuPd_3$ as a function of temperature.

## III. RESULTS

### A. Cubic $NpPd_3$

The magnetic susceptibility of cubic $NpPd_3$ as a function of temperature is shown in Fig. 1. The peak near 55 °K is indicative of antiferromagnetic ordering at this temperature. The susceptibility obeys a Curie-Weiss law in the range 100–300 °K, with an effective paramagnetic moment of $\mu = (2.74 \pm 0.03)\ \mu_B$/formula unit (F.U.) and a paramagnetic Curie temperature of $\Theta_p = -(16 \pm 4)$ °K. The ratio $\chi(T=0)/\chi(T=T_N) = 0.42$, where $\chi$ is the magnetic susceptibility and $T_N$ is the Néel temperature. Thus this ratio is well below the value of $\frac{2}{3}$ for an ideal antiferromagnet.

The electrical resistivity as a function of temperature is shown in Fig. 2. The extremely sharp anomaly at 54 °K correlates well with the peak in the susceptibility at the Néel temperature. In the range 1.75–40 °K the data fit the following relation:

$$\rho = \rho_0 + AT^5 J_5(\Theta/T) + BT^4 e^{-\Delta/kT}, \qquad (1)$$

where the three terms on the right are, respectively, the residual resistivity, $\rho_0$; the Bloch-Grüneisen phonon contribution, $\rho_p$; and the resistivity due to spin-wave scattering, $\rho_m$. Since five parameters are present in Eq. (1), care was taken to determine them in a systematic fashion. The following procedure was employed. (a) The residual resistivity was determined experimentally. (b) Up to 15 °K, $\rho - \rho_0 = 4.778 \times 10^{-6} T^5$ with a standard deviation of 0.063 $\mu\Omega$ cm. In the low-temperature limit $J_5(\infty) = 124.4$, where $J_5$ is a Debye integral. Hence, $A = 3.489 \times 10^{-8}\ \mu\Omega\,\text{cm}/°\text{K}^5$. (c) Above 15 °K the measured resistivity increases more slowly than $T^5$. This result implies that magnetic scattering is negligible near 20 °K and that $\Theta$, the Debye temperature, must be obtained to approximate the phonon resistivity above 15 °K, The asymptotic ex-

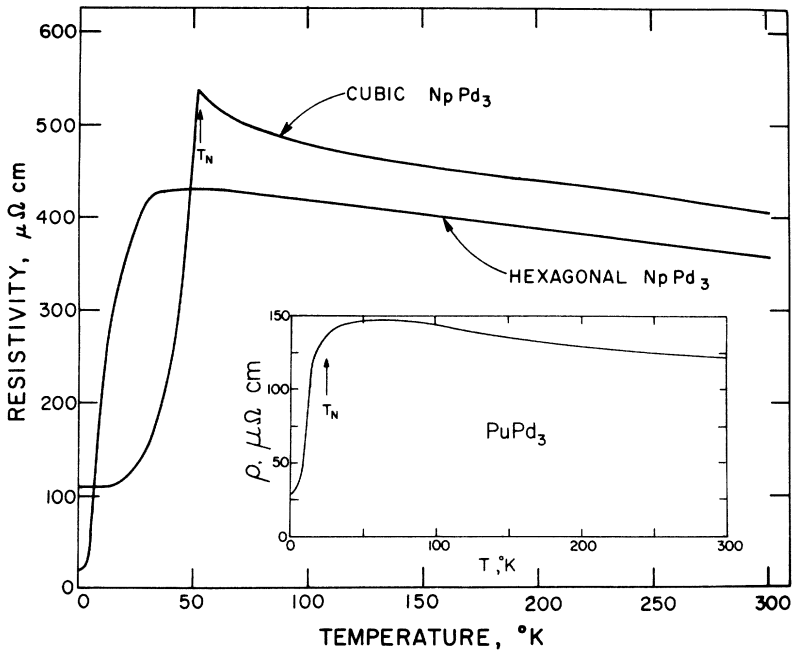


FIG. 2. Electrical resistivities of two phases of $NpPd_3$ and of $PuPd_3$ as a function of temperature.

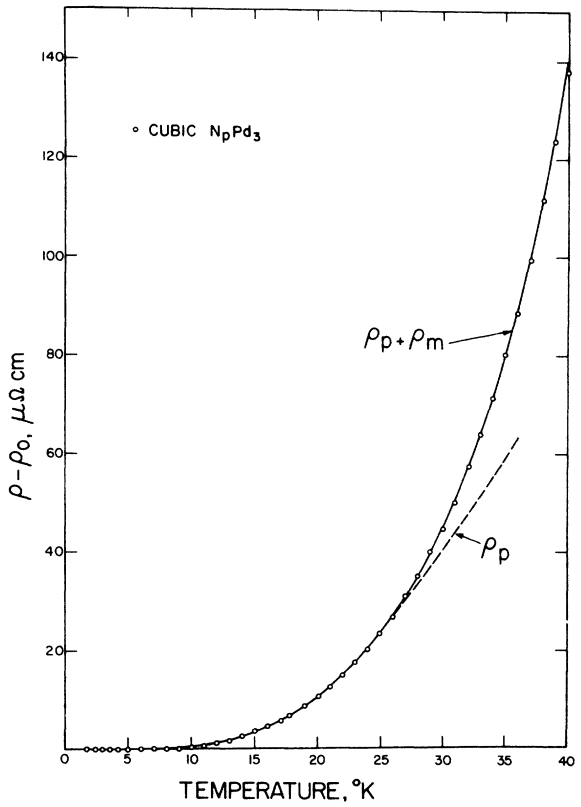


FIG. 3. Electrical resistivity of cubic $NpPd_3$ in the range 1.75–40 °K. The circles are data points. The solid line is the result of fitting the data to Eq. (1); $\rho_p$ is the phonon resistivity, which is the sole source of the temperature dependence below 25 °K; $\rho_m$ is the resistivity due to spin-wave scattering.

pansion for $J_5(x)$ given by Wilson[18] was used to estimate Θ. For the temperature range of interest ($T \simeq 20$ °K) and a reasonable Debye temperature ($\Theta \simeq 200$ °K), $x \equiv \Theta/T \simeq 10$ and

$$\rho - \rho_0 = AT^5\left[J_5(\infty) - \frac{x^5}{e^x - 1} - 120e^{-x} \times\left(1 + x + \frac{x^2}{2!} + \frac{x^3}{3!} + \frac{x^4}{4!}\right)\right]. \quad (2)$$

Equation (2) was solved numerically for $x$ at $T = 19$ °K, with the result that $\Theta = 140$ °K. The phonon resistivity up to 40 °K was then obtained graphically using the numerical tables for $J_5(x)$.[18] Thus, below 25 °K the first two terms in Eq. (1) fit the data well, as shown in Fig. 3. (d) In the range 28–38 °K, $\rho - (\rho_0 + \rho_p)$ was fitted to the third term of Eq. (1). This temperature dependence is appropriate for spin-wave scattering in an antiferromagnet with an energy gap Δ in the spin-wave dispersion relation.[19] The results are $B = 1.18 \times 10^{-3}$ μΩ cm/°K$^4$, and $\Delta/k = 160$ °K. The fit is shown in Fig. 3. The calculated curve increases faster than the experimental curve above 40 °K.

A time dependence was observed in the low-temperature data. The resistivity was remeasured six months after the original measurements, which are illustrated in Fig. 2. Because of excessive scatter in the earlier run, the new data were used in the analysis of Eq. (1) and are illustrated in Fig. 3. The second run showed that the residual resistivity had increased from 110 to 147 μΩ cm. The difference between the new and old data decreases to zero as the temperature increases to $T_N$. In view of the large residual resistivity, the deviation from Matthiesen's rule is not surprising. Some of the change in the low-temperature resistivity, which is evident after storage for many months at room temperature, may be caused by the cubic phase slowly transforming to the equilibrium hexagonal phase.

Several criticisms are therefore appropriate to the above resistivity analysis. The Debye temperature Θ is somewhat lower than expected for this brittle material with a high melting point (~1500 °C). However, in the absence of any other information on the phonon spectrum, the value Θ = 140 °K should be a reasonable order-of-magnitude

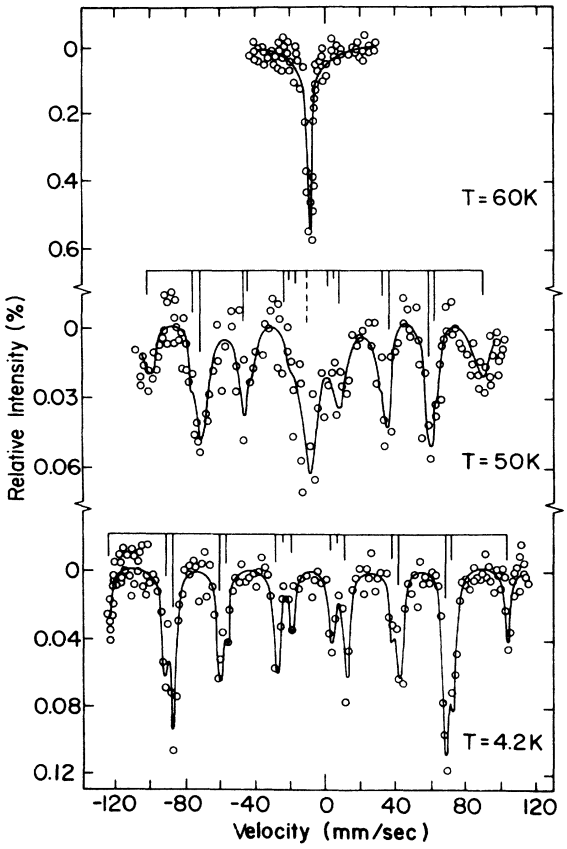


FIG. 4. Mössbauer spectra of cubic $NpPd_3$.

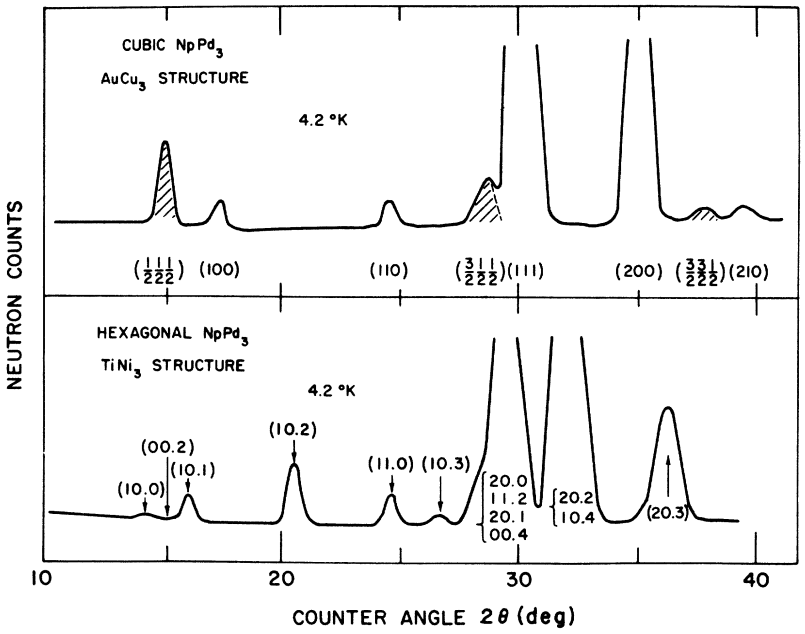


FIG. 5. Neutron-diffraction patterns of cubic and hexagonal $NpPd_3$ at 4.2 °K. The peaks due to antiferromagnetic ordering in the cubic compound are shaded.

estimate. The result $\Delta/k = 160\,^{\circ}\mathrm{K} \simeq 3T_N$, is considerably higher than expected. In this regard, the Mössbauer and neutron-diffraction data presented below indicate that the sublattice magnetization is essentially constant up to 50 °K, and suggest that the magnetic transition in cubic $NpPd_3$ is of first order. In this case, the sublattice magnetization changes discontinuously at $T_N$, and an energy gap comparable to the Néel temperature is not unreasonable. Finally, there is the question of whether the resistivities due to various scattering mechanisms are additive, since the resistivity of cubic $NpPd_3$ does not obey Matthiessen's rule. The best argument in favor of the additive resistivities is the excellent fit to the data in the temperature range in which the Mössbauer effect and neutron-diffraction data suggest that spin waves should be present.

The slope of the resistivity-temperature curve is negative above $T_N$ and suggests spin-flip scattering from neptunium localized spins. The data in the range 100–300 °K were fitted to two expressions, $\rho = A + BT + C \ln T$ and $\rho = D + ET + F/T$, where presumably the constant terms are composed of spin-disorder and residual contributions, the $T$ terms are due to phonon scattering, and the $\ln T$ and $T^{-1}$ terms are due to spin scattering. The latter two dependences have been proposed for Kondo-type[20] and spin-fluctuation[21,22] scattering. The fits give negative coefficients for the phonon resistivity in both cases, and the fitting parameters are sensitive to the temperature interval employed. Thus the significance of the results is unclear.

Mössbauer spectra for cubic $NpPd_3$ at various temperatures are shown in Fig. 4. A magnetic transition is clearly seen between 50 and 60 °K. Solid lines are fitted curves, assuming commensurate magnetic-hyperfine field and electric-field gradients. Line positions corresponding to the derived hyperfine parameters are shown by bar diagrams in the figure. At 4.2 °K one obtains a magnetic hyperfine field $H_{hf} = 3760 \pm 40$ kOe, an electric quadrupole interaction parameter $e^2qQ = 0.06 \pm 0.01$ MHz, and an isomer shift of $-22.0 \pm 0.5$ mm/sec with respect to $NpAl_2$. If we presume that the relationship between the hyperfine field and the electronic moment is similar to that observed in the neptunium monopnictides,[23] then the magnitude of the hyperfine field implies a saturation moment of $(1.95 \pm 0.10)\ \mu_B$ in cubic $NpPd_3$. At 50 °K ($T/T_N = 0.91$), the hyperfine field is reduced to only 85% of its saturation value. This implies a sharp transition between the paramagnetic and antiferromagnetic states and suggests that the transition is first order. In addition to the magnetically split spectrum at 50 °K, one also sees a small paramagnetic component. Such a situation is characteristic of Mössbauer spectra near first-order transitions and is caused by a small distribution of transition temperatures due to local imperfections in the material. Customarily, as the temperature is raised, one observes an increase in the intensity of the paramagnetic component at the expense of the split pattern, but with no significant changes in line positions. Such behavior has been observed for cubic $NpPd_3$ by Gal *et al.*[24]

The neutron-diffraction pattern of cubic $NpPd_3$ is shown in the upper half of Fig. 5. The shaded peaks are not observed above $T_N$, and are present

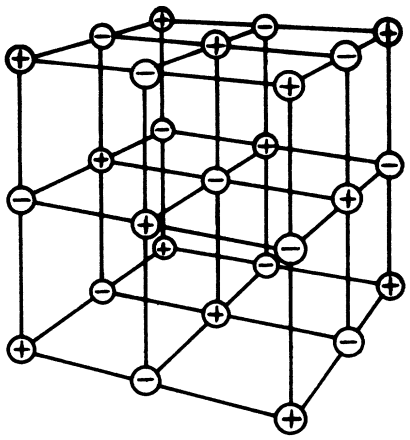

FIG. 6. Simple-cubic sublattice occupied by neptunium atoms in cubic $NpPd_3$. Plus and minus signs indicate antiferromagnetic structure. Moment directions are probably parallel to cube edge.

at low temperature because of the ordered arrangement of neptunium magnetic moments. The nuclear peaks (integer indices in Fig. 5) are, for example, either strong face-centered lines (111), (200) or weak superlattice lines (100), (110). Such an arrangement is characteristic of the $AuCu_3$ structure, in which the strong face-centered lines have a structure factor $b_{Np}+3b_{Pd}$, and the superlattice lines have a structure factor $b_{Np}-b_{Pd}$. If the atoms are distributed randomly over the two sites, the superlattice lines will be absent. From an analysis of the intensities at 78 °K, the order parameter $S$, defined as the fraction of atoms located on their ordered sites, is $0.92\pm0.03$. This is a high value for the ordering parameter, if we recall that the material must be quenched from the melt to retain the cubic phase. At temperatures below 55 °K, the neptunium magnetic moments are arranged in an antiferromagnetic structure that requires a doubling of the chemical unit cell in the three ⟨100⟩ directions. The magnetic structure may be described as consisting of ferromagnetic (111) planes coupled antiferromagnetically, and is illustrated in Fig. 6. From a consideration of the relative integrated intensities of the magnetic peaks at 4.2 °K the magnetic moments probably point along a cube edge.[25]

The magnitude of the ordered moment at 4.2 °K is $(2.0\pm0.1)\ \mu_B$/Np atom, in agreement with the hyperfine-field result. By measuring the temperature dependence of the $(\frac{1}{2}\ \frac{1}{2}\ \frac{1}{2})$ magnetic peak, the Néel temperature was determined as $(55\pm1)$ °K, which is in excellent agreement with all other measurements. The temperature dependence of this peak also indicated that the paramagnetic-antiferromagnetic transition may be first order. The intensity remained unchanged from 5 to 45 °K, falling to ~0.73 of this value at 50 °K. Since the neutron intensity is proportional to the square of the magnetic moment, the value of the latter at 50 °K is 85% of the ordered moment, in excellent agreement with the hyperfine-field result.

### B. Hexagonal $NpPd_3$

The magnetic properties of hexagonal $NpPd_3$ are quite different from those of the cubic compound, and it is worthwhile at this point to review the structural differences between the $AuCu_3$-type and the $TiNi_3$-type crystal structure. The space group of the $AuCu_3$ ($L1_2$) structure is $Pm3m$. The actinide-series ($A$) atoms are at the corners of the cube, and the Pd atoms are at the centers of each cube face. If the atom species is neglected, the packing along the ⟨111⟩ direction of the resultant face-centered-cubic cell may be characterized by $ABCABC\ldots$. The hexagonal phase of $APd_3$ has the $TiNi_3$ ($D0_{24}$) structure. This has hexagonal symmetry with space group $P6_3/mmc$ and four formula units per unit cell. The $A$ atoms are 2 $A$ in $2a$ $000$, $00\frac{1}{2}$; and 2 $A$ in $2c$ $\frac{1}{3}\frac{2}{3}\frac{3}{4}$, $\frac{2}{3}\frac{1}{3}\frac{1}{4}$. The Pd atoms are 6 Pd in $6g$ $\frac{1}{2}00$, $0\frac{1}{2}0$, $\frac{1}{2}\frac{1}{2}0$, $\frac{1}{2}0\frac{1}{2}$, $0\frac{1}{2}\frac{1}{2}$, $\frac{1}{2}\frac{1}{2}\frac{1}{2}$; and 6 Pd in $6h$ $x2x\frac{1}{4}$, $2\bar{x}\bar{x}\frac{1}{4}$, $x\bar{x}\frac{1}{4}$, $\bar{x}2\bar{x}\frac{3}{4}$, $2xx\frac{3}{4}$, $\bar{x}x\frac{3}{4}$. The value of $x$ is $\sim\frac{1}{6}$. Although this atomic structure appears complicated, examination, again without regard to atomic species, shows that the $ABCABC\ldots$ packing of the cubic structure is now changed to $ABACABAC\ldots$ along the ⟨111⟩ direction. This is the double-hexagonal close-packed structure of, for example, elemental praseodymium and neodymium. Of course, arguments with regard to packing are exact only if the $c/a$ ratio is ideal ($c/a=\frac{8}{3}\sqrt{\frac{8}{3}}=1.633$), but the experimental values for $UPd_3$ and $NpPd_3$ of 1.672 and 1.655, respectively, show that ideal packing is almost achieved. Following the analogy with praseodymium metal, we may describe the exact configuration of the nearest neigh-

TABLE I. Comparison of the atomic environment of actinide ($A$) atoms in the cubic ($AuCu_3$ structure) and hexagonal ($TiNi_3$ structure) phases of $APd_3$. The cubic and hexagonal notation in the $TiNi_3$ structure refers to the detailed configuration of the nearest neighbors. The range of distances apply to the hexagonal structure only.

| | | $TiNi_3$ Structure | |
|---|---|---|---|
| Distance (Å) | $AuCu_3$ Structure | $2a$ site (cubic) | $2c$ site (hex.) |
| 2.88–2.91 | 12 Pd | 12 Pd | 12 Pd |
| 4.18 | 6 $A$ | 6 $A$ | 6 $A$ |
| 4.77 | ··· | 2 $A$ | ··· |
| 4.99–5.05 | 24 Pd | 18 Pd | 24 Pd |
| 5.58 | ··· | 12 Pd | ··· |
| 5.77–5.82 | 12 $A$ | 6 $A$ | 12 $A$ |

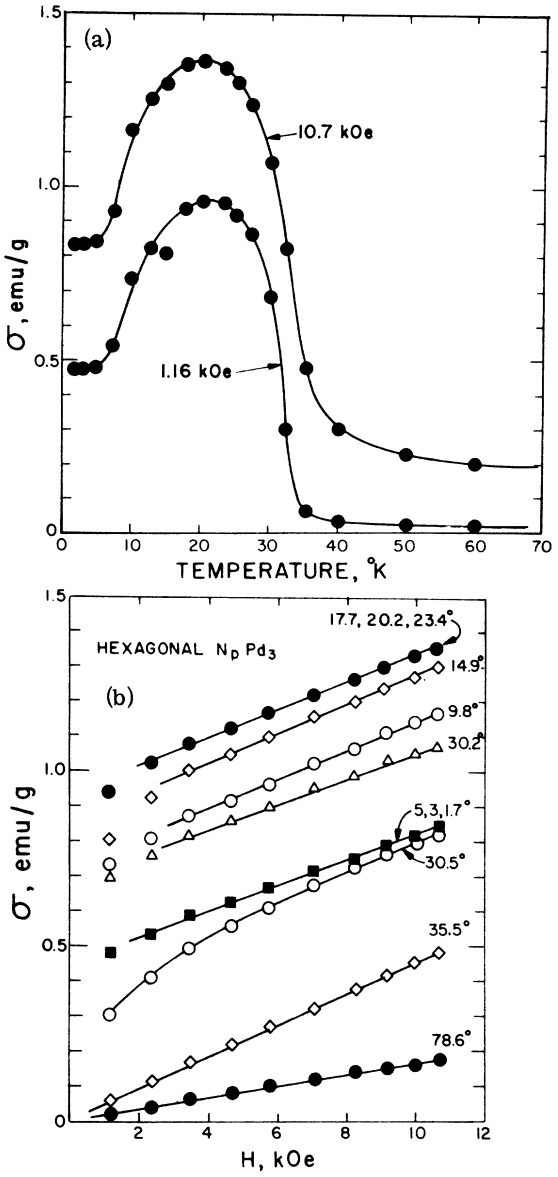


FIG. 7. Magnetization of hexagonal $NpPd_3$. (a) Magnetization as a function of temperature at applied magnetic fields at 1.16 and 10.7 kOe. (b) Magnetization as a function of applied magnetic field at various temperatures.

bors of the $A$ atom as either cubic ($2a$ sites or $A$ layers) or close-packed hexagonal ($2c$ sites or $B$ and $C$ layers). The coordination numbers and distances are given for the two sites in Table I. Clearly, the two structures are closely related.

Isofield-magnetization–temperature ($\sigma$-$T$) curves of hexagonal $NpPd_3$ are shown in Fig. 7(a). These curves are characterized by a temperature-independent range as $T \to 0$ °K, a broad peak near 20 °K, and a sharp drop in magnetization between 20 and 35 °K. Isotherms ($\sigma$-$H$ curves) for the low-temperature magnetization are shown in Fig. 7(b). The $\sigma$-$H$ curves do not exhibit any saturation behavior, even at 1.74 °K, and the high-field susceptibility (as judged by the slope of $\sigma$-$H$ for $6 < H < 12$ kOe) is almost independent of temperature for $T < 32$ °K. The spontaneous moment, obtained by extrapolation of the $\sigma$-$H$ curve at 1.74 °K to $H = 0$, is 0.05 $\mu_B$/F.U., and the maximum moment induced at 12 kOe is 0.14 $\mu_B$/F.U. Above 6 kOe the magnetization can be represented by $\sigma = \sigma_0 + \chi H$. Plots of $\sigma_0$ versus $T$ extrapolate to zero at an "ordering" temperature of ~35 °K. In addition, plots of $\sigma^2$ versus $H/\sigma$ for low fields ($H < 4$ kOe) indicate an "ordering temperature" of (32 ± 1) °K. Hence the magnetization results imply some sort of magnetic ordering near 32 °K in this material. At higher temperatures, the $\sigma$-$H$ curves are linear at all fields, and the susceptibility in the range 100–300 °K obeys a Curie-Weiss law with an effective paramagnetic moment of $\mu_{eff} = (2.75 \pm 0.03)\ \mu_B$/F.U., and a paramagnetic Curie temperature of $\Theta_p = -42 \pm 2$ °K.

Considerable effort was expended on hexagonal $NpPd_3$ to ensure that the magnetization results were not sample dependent. Similar results were obtained from a sample made from independent batches of neptunium and palladium. The results were also reproduced after a two-week anneal of a hexagonal specimen at 800 °C. In addition, field cooling had no effect on the magnetization results.

The electrical resistivity of hexagonal $NpPd_3$ is shown in Fig. 2. The resistivity increases from its residual value as $\rho = 19.72 + 0.1778T^3$ with a standard deviation of 0.2 $\mu\Omega$ cm in the range 1.24–4.93 °K. Deviations from this dependence are positive up to 10 °K and negative thereafter. The resistivity increases rapidly up to a knee near 30 °K, and the slope drops by a factor of 6 abruptly at 32 °K, i.e., near the temperature at which the magnetization results indicate some sort of ordering. At higher temperatures, the slope of the resistivity-temperature curve is negative, and the curves for the two phases are nearly parallel. The high-temperature hexagonal data were fitted to the same two functions as the cubic data, with similar results. The rapid increase in the resistivity as the temperature increases from 0 °K is presumably due to spin-disorder scattering. The $T^3$ dependence is probably due to this scattering mechanism, since the initial phonon resistivity is small in the cubic compound and, as discussed below, the hexagonal phase does not possess long-range order.

Mössbauer-effect spectra for hexagonal $NpPd_3$ are shown in Fig. 8. Near the transition temperature of 30 °K, the paramagnetic line begins to broaden and continues to do so as the temperature is lowered. At 4.2 °K some structure is apparent, but no well-defined hyperfine pattern is seen. In the $TiNi_3$ structure, two neptunium inequivalent

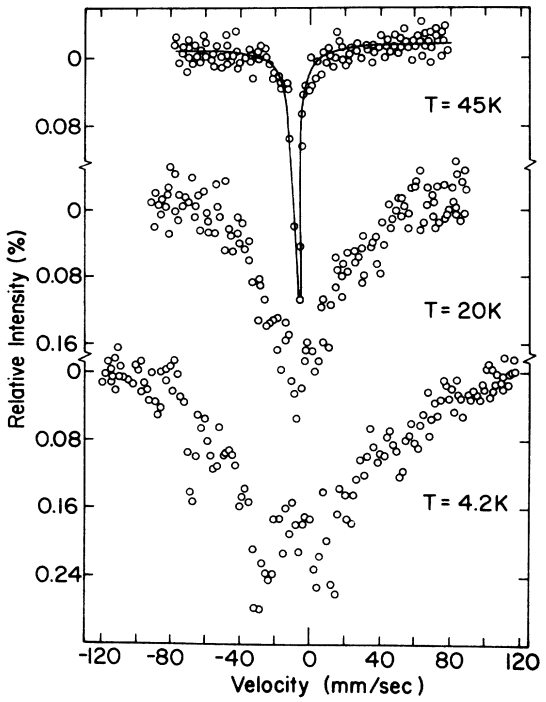


FIG. 8. Mössbauer spectra of hexagonal $NpPd_3$ illustrating the low-temperature broadening of the paramagnetic line.

sites are available; therefore, two hyperfine patterns could be present. However, an attempt to fit the data assuming two sites was not successful. Although line broadening does begin near the apparent transition temperature (~32 °K), it cannot be ascribed to a simple magnetic transition. For example, at 20 °K we would anticipate a hyperfine field of at least 70% saturation. Since the paramagnetic moment is 2.7 $\mu_B$, we would expect an ordered moment of ~2 $\mu_B$, and therefore hyperfine splittings comparable to those shown in Fig. 4. In contrast, however, the line has only broadened to about ten times the paramagnetic width. Since the over-all broadening at 4.2 °K covers a velocity range comparable to that of the cubic case, it is clear that magnetic moments of comparable magnitude are involved (~1–2 $\mu_B$). The Mössbauer data eliminate the possibility of a magnetic transition with a small magnetic moment and the possibility that impurity effects dominate the magnetization results. The observed spectra may be due either to paramagnetic relaxation with a spin-relaxation time of $\sim 10^{-10}$–$10^{-11}$ sec or to a large distribution in hyperfine fields that might occur in the presence of pronounced short-range order.

Finally, the neutron-diffraction pattern of hexagonal $NpPd_3$ at 4.2 °K is shown in the lower half of Fig. 5. The patterns at 78 and 4.2 °K are *identical*; therefore, no magnetic transition has been observed with neutron diffraction. The intensities can be accounted for accurately by using coherent scattering lengths[26] of $b_{Np} = 1.055 \times 10^{12}$ cm and $b_{Pd} = 0.60 \times 10^{-12}$ cm and the $TiNi_3$ structure described above. Based on considerations of a number of possible antiferromagnetic structures (particularly the one observed for cubic $NpPd_3$; see above), we estimate that the upper limit of any ordered magnetic moment in a long-range antiferromagnetic structure is ~0.5 $\mu_B$/Np atom.

### C. $PuPd_3$

The magnetic susceptibility and electrical resistivity of $PuPd_3$ have been reported previously[27,28] and are included here for completeness. The magnetic susceptibility as a function of temperature is shown in Fig. 1. The peak at 24 °K indicates antiferromagnetic ordering at this tempera-

TABLE II. Magnetic properties of $APd_3$ compounds. $V/Z$ is the volume per formula unit, $\chi_m$ is the molar susceptibility, $\mu_{eff}$ is the effective paramagnetic moment, $\Theta_p$ is the paramagnetic Curie temperature, $\rho$ is the electrical resistivity, $T_N$ is the Néel temperature, $\mu_{sat}$ is the ordered moment at 5 °K, and $H_{hf}$ is the hyperfine field at 5 °K.

| Compound | Lattice (Å) | $V/Z$ (Å$^3$) | $\chi_m$ (300 °K) ($10^{-4}$ emu/mole) | $\mu_{eff}$ ($\mu_B$/F. U.) | $\Theta_p$ (°K) | $\rho$ (300 °K) ($\mu\Omega$ cm) | $T_N$ (°K) | $\mu_{sat}$ ($\mu_B$/A) | $H_{hf}$ (kOe) |
|---|---|---|---|---|---|---|---|---|---|
| $UPd_3$ $TiNi_3$ type | $a = 5.770$ $c = 9.648$ | 69.54 | 36[a] | 2.6[a] | ~0[a] | ... | ... | ... | ... |
| $NpPd_3$ $TiNi_3$ type | $a = 5.767$ $c = 9.544$ | 68.72 | 28 | 2.75 ± 0.03 | −42 ± 2 | 358 | ~32? | < 0.5 | ... |
| $NpPd_3$ $AuCu_3$ type | $a = 4.095$ | 68.67 | 30 | 2.74 ± 0.03 | −16 ± 4 | 410 | 55 ± 1 | 2.0 ± 0.1 | 3760 ± 40 |
| $PuPd_3$ $AuCu_3$ type | $a = 4.105$ | 69.18 | 5 | 1.0 ± 0.1 | −34 ± 2 | 122 | 24 + 2 | 0.8 ± 0.1 | ... |

[a]Reference 10.

ture. The resistivity is shown in Fig. 2, and the general shape is similar to that of hexagonal $NpPd_3$. The main difference in these two materials is that $PuPd_3$ orders magnetically, although no sharp knee is seen in the resistivity data. The Néel temperature is about one-half the temperature at which the maximum occurs in the resistivity-temperature curve.

Neutron-diffraction patterns of $PuPd_3$ demonstrate that below ~24 °K the material is antiferromagnetic with the same magnetic structure as found in cubic $NpPd_3$ (Fig. 6). The ordered moment at 4.2 °K is $(0.8 \pm 0.1)$ $\mu_B$/Pu atom. The effective paramagnetic moment (see Table II) is $(1.0 \pm 0.1)$ $\mu_B$/F.U. In principle, the order parameter $S$ for cubic $PuPd_3$ can also be obtained from the intensities of the neutron-diffraction patterns. In practice, however, the quantity obtained is the product of the order parameter and the coherent scattering length of $^{239}$Pu. Assuming $b_{Pd} = 0.60 \times 10^{-12}$ cm, this product is $(0.85 \pm 0.04) \times 10^{-12}$ cm. Reference 26 gives $b_{^{239}Pu} = 0.75 \times 10^{-12}$ cm, but, since the maximum value of $S$ is unity, this value of $b_{^{239}Pu} = 0.75 \times 10^{-12}$ cm must be too low. Few experiments have been attempted using the $^{239}$Pu isotope with its high absorption cross section, and our result may well be the best so far. Unfortunately, these uncertainties do not allow a precise definition of the order parameter in cubic $PuPd_3$.

## IV. DISCUSSION

The most striking result of this investigation is the difference in magnetic behavior between cubic and hexagonal $NpPd_3$, despite the similar environment of the neptunium atoms in both crystal structures. Antiferromagnetic ordering below $T_N = 55$ °K is well documented for cubic $NpPd_3$. In addition, the essentially constant value of the sublattice magnetization up to 50 °K, as observed by the Mössbauer and neutron-diffraction experiments, provide strong evidence that the magnetic transition is of first order. Further, the resistivity data suggest that spin waves exist up to temperatures close to $T_N$. This result is also consistent with the sublattice-magnetization data, which yield a moment equal to the saturation moment up to ~20 °K, the temperature range dominated by the phonon resistivity, and a moment which decreases by only 4% from the saturation value in the range 20–40 °K, the temperature region in which the magnetic scattering appears.

In contrast, hexagonal $NpPd_3$ does not possess long-range magnetic order. The neutron-diffraction results indicate that the ordered moment in this structure is less than ~0.5 $\mu_B$/Np, whereas the Mössbauer effect yields a neptunium moment of 1–2 $\mu_B$ at 4.2 °K. We believe that the most appropriate model for the hexagonal compound is one of short-range magnetic order distributed throughout the bulk. This model is consistent with the broadening of the paramagnetic Mössbauer line and the rapid decrease in the total resistivity that takes place as the temperature is lowered below ~30 °K. The model can also explain the maximum in the $\sigma$-$T$ curves if one assumes that the short-range order is antiferromagnetic in nature, which is reasonable since $\Theta_p$ is negative. Near the short-range ordering temperature an external magnetic field would be able to overcome the antiferromagnetic spin correlations, and an increase in magnetization would be expected. However, as the temperature approaches 0 °K, the spins tend to lock in antiferromagnetically, and the magnetization would decrease giving rise to a broad maximum in the $\sigma$-$T$ curve.

The contrasting results for the two phases are probably due to the details of the crystal-field and exchange interactions. As discussed in the Introduction, the $A$-$A$ distances are large in the $TiNi_3$ and $AuCu_3$ structures (see Table I), and we should expect the crystal-field interactions to be important, as is the case in the rare-earth–$Pd_3$ series.[8] A prerequisite for attempting crystal-field calculations is to determine the number of $f$ electrons on the actinide ion. Wernick *et al.*[10] and Davidov *et al.*[11] have assumed $5f^2$, and hence a $U^{4+}$ ionic state in $UPd_3$. This is consistent with $ThPd_3$, which is diamagnetic, and hence $Th^{4+}$. If the crystal-field splitting is less than ~300 °K, the effective moment in the paramagnetic state should be an indication of the $f$-electron configuration. For two, three, four, and five $f$ electrons, the free-ion Russell-Saunders values of $\mu_{eff}$ are 3.58, 3.62, 2.68, and 0.85 $\mu_B$, respectively. The value of $\mu_{eff}$ for $UPd_3$ is 2.6 F.U., although for low concentrations of uranium in $ThPd_3$ the value[10] is 3.35 $\mu_B$/U atom. Therefore the situation in $UPd_3$ is ambiguous, and this and other measurements[11] indicate that the crystal-field model is inadequate. On the other hand, for $PuPd_3$ the values of $\mu_{eff}$ and $\mu_{sat}$ are 1.0 and 0.8 $\mu_B$, respectively, and are close to the values of 0.85 and 0.71 $\mu_B$ for the free-ion $5f^5$ configuration. The slight increase over the free-ion values may be caused by $J$ mixing, which is known to be serious for the $5f^4$ and $5f^5$ configurations.[29] A $5f^5$ configuration for $PuPd_3$ implies an ionic state of $Pu^{3+}$, the same ionization state observed for all the rare-earth series with the $AuCu_3$ structure.[8] In the case of $NpPd_3$, the $\mu_{eff}$ value is 2.75 $\mu_B$, compared with a theoretical value of 2.68 $\mu_B$ for the $5f^4$ configuration. Accordingly, we have assumed $Np^{3+}$ ($5f^4$) for both hexagonal and cubic $NpPd_3$. Note that the values of $\mu_{eff}$ and $V/Z$ (see Table II) are the same for both phases, so that different $f$ configurations cannot be justified. Thus, for cubic $NpPd_3$ ($J = 4$, $5f^4$), the crystal-field

ground state in the familiar notation of Lea, Leask, and Wolf[30] depends on the values of the parameters $W$, a measure of the over-all crystal-field strength, and $x$, a measure of the ratio between the fourth- and sixth-order terms. Basing our initial considerations on a point-charge model in which both the 12 nearest neighbors (Pd) with negative charge and the six next-nearest neighbors (Np) with positive charge contribute to the crystal-field potential,[8,9] $W$ is negative and $x$ is positive. The ground state is the singlet $\Gamma_1$ if the fourth-order term dominates the crystal field, which is usually the case; otherwise, the ground state is the $\Gamma_3$ doublet. Both these eigenstates are nonmagnetic. We have not, however, considered the exchange interaction which may well dominate the crystal field and cause the ground state to support a magnetic moment. By postulating, at least temporarily, a nonmagnetic ground state for the Np ion in this coordination, we may readily develop a qualitative explanation for the magnetic behavior of both the cubic and hexagonal phases of $NpPd_3$. For the cubic compound, the exchange interaction is sufficient to overcome the crystal field, and the ordering is a first-order transition similar to the mechanism discussed by Blume[31] for the $5f^2$ configuration. In the hexagonal compound, the nonideal value of $c/a$ implies that a second-order term $V_2$ is introduced into the crystal-field potential. This increases the over-all crystal-field splitting so that the exchange cannot cause spontaneous ordering. Such a theory is quantitatively successful in explaining the magnetic behavior of both double-hexagonal close-packed and face-centered cubic praseodymium.[32] Unfortunately, both the magnetization and the Mössbauer results obtained for hexagonal $NpPd_3$ argue strongly against the singlet–ground-state model being correct. If a singlet ground state were present in $NpPd_3$ the low-temperature susceptibility would be independent of temperature, and the *susceptibility* (not the magnetization) would resemble Fig. 7(a). A maximum in the susceptibility at intermediate temperatures can arise from the interaction of the exchange with a singlet–ground-state system,[14,32] but Fig. 7 illustrates that the behavior is more complex in this material. At the lowest temperatures, the Mössbauer spectra would also be simple and essentially exhibit no magnetic behavior. The behavior observed in Fig. 7 cannot be explained on the basis of a nonmagnetic ground state, even if spin-relaxation effects are considered. Hence, a simple approach involving a single-$J$ ground state and first- and second-nearest neighbors fails to explain the magnetic behavior of both $NpPd_3$ phases.

The precise nature of the short-range order in hexagonal $NpPd_3$ is at present unknown. However, the change in slope in the resistivity at 32 °K and the abrupt increase in the low-field (1-kOe) magnetization below $\simeq 35$ °K [Fig. 7(a)] imply that the onset of this order occurs in a narrow temperature range of a few degrees. One possibility, therefore, is that a small concentration of magnetic clusters are distributed throughout the specimen, and that they all order antiferromagnetically at nearly the same temperature. They would be finite in extent and thus present a net magnetization to the surrounding neptunium moments. Presumably, the onset of this cluster ordering would polarize the surrounding neptunium moments and thus influence the properties of the bulk. Neptunium moments surrounding the clusters would experience a local internal field dependent on the distance from the clusters. The resultant distribution of internal fields could account for the Mössbauer line broadening below ~30 °K. The origin of such clusters could be a small concentration of stacking faults that persist even after heat treatment in specimens close to stoichiometry. Since the $TiNi_3$-type structure is a four-layer structure, it does seem possible for a small number of atoms to occupy the wrong sites. In principle, short-range antiferromagnetic correlations can be observed by neutron diffraction as broad peaks at the positions of incipient superlattice reflections. However, in the present experiment with such a small polycrystalline sample, the failure to observe any such peaks is not conclusive.

Short-range magnetic order accounts adequately for the magnetization, resistivity, and Mössbauer-effect measurements in hexagonal $NpPd_3$. In cubic $NpPd_3$ any possible spin fluctuations are quenched below $T_N$. Hence all the measurements are consistent with long-lived neptunium moments, and no evidence exists for spin fluctuations in either phase of $NpPd_3$. This result is in contrast to other actinide materials, in which the moment is not long lived, and for which the localized spin-fluctuation model has been quite successful.[2,28,33] In particular, spin fluctuations are manifested in the electrical resistivity of $ARh_3$ compounds, all with the $AuCu_3$-type structure, as the $5f$ band stabilizes a magnetic moment in going across the series from thorium to plutonium.[34]

## ACKNOWLEDGMENTS

The authors wish to thank D. J. Lam, A. T. Aldred, and A. J. Arko for several stimulating discussions. Thanks are also due to G. J. Schlehman for assistance in sample preparation and to J. E. Mapoles and R. L. Panosh for assistance in making the Mössbauer-effect and magnetization measurements, respectively. One of us (W.J.N.) would like to thank Monmouth (Illinois) College for the use of the computing facilities.

*Work performed under the auspices of the U. S. Atomic Energy Commission.

†Present address: Lawrence Livermore Laboratory, Livermore, Calif. 94550.

‡Present address: Uniroyal, Inc., Research Center, Middlebury, Conn. 06749.

[1]D. D. Koelling, A. J. Freeman, and G. O. Arbman, Nucl. Metall. 17, 194 (1970).

[2]A. J. Arko, M. B. Brodsky, and W. J. Nellis, Phys. Rev. B 5, 4564 (1972).

[3]H. H. Hill, Nucl. Metall. 17, 2 (1970).

[4]See, for example, Y. L. Wang and B. R. Cooper, Phys. Rev. B 2, 2607 (1970); P. Fulde and I. Peschel, Advan. Phys. 21, 1 (1972), and references therein.

[5]W. J. Nellis and M. B. Brodsky, Phys. Rev. B 4, 1594 (1971).

[6]G. H. Lander, M. B. Brodsky, B. D. Dunlap, W. J. Nellis, and M. H. Mueller, Bull. Am. Phys. Soc. 17, 338 (1972); W. J. Nellis and M. B. Brodsky, Bull. Am. Phys. Soc. 16, 326 (1971).

[7]W. J. Nellis, A. E. Dwight, and H. W. Knott, J. Appl. Cryst. 5, 306 (1972), and references therein.

[8]W. E. Gardner, J. Penfold, T. F. Smith, and I. R. Harris, J. Phys. 2, 133 (1972).

[9]I. Nowik, B. D. Dunlap, and G. M. Kalvius, Phys. Rev. B 6, 1048 (1972).

[10]J. H. Wernick, H. J. Williams, D. Shaltiel, and R. C. Sherwood, J. Appl. Phys. 36, 982 (1965).

[11]D. Davidov, H. Lotem, D. Shaltiel, M. Weger, and J. H. Wernick, Phys. Rev. 184, 481 (1969).

[12]D. Davidov (private communication).

[13]K. H. J. Buschow and H. J. van Daal, AIP Conf. Proc. 5, 1464 (1972).

[14]J. Mulak and A. Misiuk, Bull. Acad. Polon. Sci. Ser. Chim. 19, 207 (1971); J. Leciejewicz and A. Misiuk, Phys. Status Solidi A13, K79 (1972).

[15]M. B. Brodsky, N. J. Griffin, and M. D. Odie, J. Appl. Phys. 40, 895 (1969).

[16]J. W. Ross and D. J. Lam. Phys. Rev. 165, 617 (1968).

[17]B. D. Dunlap, G. M. Kalvius, S. L. Ruby, M. B. Brodsky, and D. Cohen, Phys. Rev. 171, 316 (1968).

[18]A. H. Wilson, *The Theory of Metals*, 2nd ed. (Cambridge U. P., London, 1965), p. 336.

[19]A. R. Mackintosh, Phys. Lett. 4, 140 (1963).

[20]F. E. Maranzana, J. Phys. Chem. Solids 31, 2245 (1970).

[21]N. Rivier and V. Zlatic, J. Phys. F 2, *L*87 (1972); N. Rivier and V. Zlatic, J. Phys. F 2, *L*99 (1972).

[22]R. Jullien, M. T. Béal-Monod, and B. Coqblin, Phys. Rev. Lett. 30, 1057 (1973).

[23]G. H. Lander, B. D. Dunlap, M. H. Mueller, I. Nowik, and J. F. Reddy, Intern. J. Mag. 4, 99 (1973).

[24]J. Gal, Z. Hadari, E. R. Bauminger, I. Nowik, and S. Ofer, Solid State Commun. 13, 647 (1973).

[25]See, for example, W. L. Roth [Phys. Rev. 110, 1333 (1958)] for a discussion of this type of magnetic structure. The observed ratio $I(\frac{1}{2}\ \frac{1}{2}\ \frac{1}{2})/I(\frac{3}{2}\ \frac{1}{2}\ \frac{1}{2}) = 1.4 \pm 0.1$; for the magnetic moments parallel to a cube edge the calculated ratio is 1.55; for the moments lying in the (111) plane the calculated ratio is 3.06.

[26]Neutron Diffraction Commission, Acta Cryst. A28, 357 (1972).

[27]W. J. Nellis and M. B. Brodsky, AIP Conf. Proc. 5, 1483 (1972).

[28]A. R. Harvey, M. B. Brodsky, and W. J. Nellis, Phys. Rev. B 7, 4137 (1973).

[29]S.-K. Chan and D. J. Lam, Nucl. Metall. 17, 219 (1970); D. J. Lam and S.-K. Chan, Phys. Rev. B 6, 307 (1972).

[30]K. R. Lea, M. J. M. Leask, and W. P. Wolf, J. Phys. Chem. Solids 23, 1381 (1962).

[31]M. Blume, Phys. Rev. 141, 517 (1966).

[32]B. D. Rainford, AIP Conf. Proc. 5, 591 (1972).

[33]S. Doniach, AIP Conf. Proc. 5, 549 (1972).

[34]W. J. Nellis, A. R. Harvey, and M. B. Brodsky, AIP Conf. Proc. 10, 1076 (1973).